A Multi-Factorial Assessment of Functional Human Autistic Spectrum Brain Network Analysis

Oswaldo Artiles, Life Senior Member, IEEE
School of Computing and Information Sciences
Florida International University
Miami, Florida
Email: {oarti001@fiu.edu}

Fahad Saeed, Senior Member, IEEE
School of Computing and Information Sciences
Florida International University
Miami, Florida
Email: {fsaeed@fiu.edu}

2021 IEEE International Conference on Bioinformatics and Biomedicine (BIBM) | 978-1-6654-0126-5/21/$31.00 ©2021 IEEE | DOI: 10.1109/BIBM52615.2021.9669679

***Abstract*—The variability of the results obtained by the statistical analysis of functional human brain networks depend on multiple factors such as: the source of the fMRI data, the brain parcellations, the graph theory measures, and the threshold values applied to the functional connectivity matrices to obtain adjacency matrices of sparse graphs. Therefore, the brain network used for down-stream analysis is heavily dependent on the methods that are applied to the fMRI data to obtain and analyze such networks. In this paper we present the preliminary results of a multi-factorial assessment of the statistical analysis of functional human brain networks. The assessment was performed in the functional human brain networks obtained from the resting state fMRI data of ten imaging sites provided by the Autism Brain Imaging Data Exchange (ABIDE) preprocessed functional magnetic resonance database, with six different functional brain parcellations, six different graph theory measures, and three different threshold values applied to the corresponding connectivity matrices to obtain sparse graphs. The statistical analysis to detect differences between the networks representing autism and control subjects were performed with four different statistical methods, using the p-values to determine the levels of significance of the analysis. Our main results show a strong dependence of functional human brain networks statistical analysis on the brain parcellations, and on the graph theory measures. Our results further show that the results of these analysis are less dependent on the statistical tests methods and on the threshold values of the sparse graphs for all practical purposes. An additional result is that the levels of significance of the statistical tests obtained for data provided by individual sites were much higher than the global levels of significance obtained by averaging the results of all the sites, implying that the best results on the analysis of functional human brain networks are obtained when the source of the fMRI data is the same for all the data. Since reproducibility and reliability of functional brain network statistical analysis is strongly dependent on the graphs obtained from fMRI data; our expectation is that the novel results presented in this paper would further help researchers in this field to develop methods that are reliable and reproducible.**

***Index Terms*—fMRI, functional brain network, graph theory, autism, statistical analysis**

I. Introduction

Functional magnetic resonance imaging (fMRI) is non-invasive imaging technique widely used in neuroscience to understand the functional connectivity of the human brain. The modeling and analysis of fMRI data with complex graph theory as functional human brain networks, known as network neuroscience [1]–[3], has been fundamental in the advances of modern neuroscience. However, the variability results of the statistical analysis of functional human brain networks depend on multiple factors such as: the sources of the fMRI data, the choice of suitable brain parcellations [4]–[7], as well as on the selected graph theory measures [8]–[10], and on the threshold values applied to the functional connectivity matrices [11], [12], to derive the adjacency matrices that represent sparse graphs. Such variability on the results of the statistical analysis, produces classification and characterization methods that may not be reliable, or reproducible for fMRI data obtained from various sources [13].

TABLE I: International Imaging Sites from ABIDE preprocessed fMRI data used in this paper [14].

International Imaging Site	Control	ASD
California Inst. Tech. (Caltech)	18	19
Kennedy Krieger Institute (KKI)	28	20
L. Maximilians U. (MaxMun)	28	24
NYU Langone Medical (NYU)	100	75
University Pittsburgh (Pitt)	27	29
Social Brain Lab (SBL)	15	15
University California LA (UCLA-1)	28	20
University Michigan (UM-1)	53	53
University Utah (USM)	25	46
Yale University (Yale)	28	28
TOTAL)	353	350

In this paper we present the preliminary results of a multi-factorial assessment of the statistical analysis of functional human brain networks. The assessment was performed in the functional human brain networks obtained from the resting state fMRI data provided by the Autism Brain Imaging Data Exchange (ABIDE) preprocessed functional magnetic resonance database [14] from the ten imaging sites shown in Table I, with six different functional brain parcellations, six different graph theory measures, and three different threshold values applied to the corresponding connectivity matrices to obtain sparse graphs. To ensure the consistency of the statistical analysis to detect differences between the networks representing autism and control subjects, four different statistical methods

were chosen for this analysis, using the corresponding p-values that determine their level of significance.

The main contribution of the paper is the implementation of methods for the assessment of the multiple factors which determine the variability of the results obtained with the statistical analysis of functional human brain networks. These methods allowed us to demonstrate that there is a strong dependence of functional human brain networks statistical analysis on the brain parcellations, and on the graph theory measures. Our results further show that the results of these analysis are less dependent on the statistical tests methods and on the threshold values of the sparse graphs for all practical purposes. An additional result is that the levels of significance of the statistical tests obtained for individual sites were much higher than the global levels of significance obtained by averaging the results of all the sites, implying that the best results on the statistical analysis of functional human brain networks are obtained when the source of the fMRI data is the same for all the data.

The rest of the paper is organized as follows: Section II describes the fMRI data and the implemented methods, Section III presents the main results, Section IV analyzes the main results, the final conclusions and future work are presented in Section V.

II. FMRI DATA AND METHODS

A. ABIDE rest-fMRI preprocessed data

The resting state fMRI data used in our experiments was obtained from the publicly available Autism Brain Imaging Data Exchange (ABIDE) preprocessed database, for the ten international imaging sites listed in Table I, with a total of 353 control and 350 autism subjects [14]. The preprocessing pipeline chosen for this data was the Configurable Pipeline for the Analysis of Connectomes (CPAC), and the filt-global preprocessing strategy, which are described in detail in the ABIDE Preprocessed website (http://preprocessed-connectomes-project.org/abide/index.html). For each site, the fMRI data for six ROI atlases were chosen, three atlases derived from fMRI data: cc200, cc400 [15], dosenbach160 [16], and three atlases derived from structural anatomic information: Automated Anatomical Labeling (aal) [17], Eickhoff-Ziles (ez) [18], and Talaraich and Tournoux (tt) [19], more information about these atlases is given in [20], [21].

B. ABIDE fMRI data processing pipeline

Figure 1 shows the pipeline implemented to perform the statistical analysis of the graph theory measures computed from the human brain functional networks representing the ABIDE fMRI preprocessed data listed in Table I. The first step in this pipeline was to compute the normalized connectivity matrices from the corresponding fMRI data for each autism and control subjects, using the Pearson correlation function available in the NumPy library (https://numpy.org). Then, the absolute values of the weights of the connectivity matrices were computed, from which two average absolute connectivity matrices were obtained for each site and for each atlas: one for the control subjects and another for the autism subjects, obtaining twelve average absolute connectivity matrices per site with normalized weights. Three threshold values: 0.1, 0.2, 0.3 were applied to the average absolute connectivity matrices resulting in adjacency matrices representing three sparse graphs for the control subjects and three for the autism subjects, obtaining thirty-six adjacency matrices per site. An undirected weighted functional graph was computed from each adjacency matrix with the algorithms available in the Networkx package [22]. Then, six graph theory measures were computed for each functional graph (details in Section II-C below). Finally, statistical analysis of the graph measures was performed for the functional graphs representing the control and autism subjects, to detect statistical differences between these two groups of fMRI data (details in Section II-D below).

C. graph theory measures

The graph theory measures implemented for the functional graphs were: normalized measure of node strength, closeness centrality, node betweenness centrality (BC), edge betweenness centrality (EBC), Rich-Club coefficient (RC), and clustering coefficient (CC). A node strength is computed as the sum of the weights of the edges attached to the node. The closeness centrality of a node is equal to the inverse of the average shortest path distance to the node. A node betweenness centrality (BC) measures the proportion of shortest paths between all pair of nodes in the graph that passes through the node, and the edge betweenness centrality is the same measure applied to the edges of the graph. The Rich-Club coefficient at each level of degree, k, is defined as the ratio of the number of edges in the subgraph comprising only nodes with degree greater than k, relative to the total possible number of edges in this subgraph. The clustering coefficient of a node is the proportion of closed triangles that are attached to the node, relative to the total number of closed triangles that are possible between the neighbors of the node. These measures were computed with the corresponding algorithms implemented in the NetworkX package. More details about these graph measures in [8], [11], [22], [23].

D. Statistical tests methods

In order to ensure the consistency of the statistical results, four statistical tests methods were used to perform the statistical analysis of the control and autism graphs measures. The chosen methods were: The parametric t-test (tt), and three nonparametric tests: the Kolmogorov–Smirnov test (kst), the Kruskal–Wallis H-test (krust), and the Mann–Whitney U test (mwt). The t-test is used to determine if the means of two sets of data are statistically different from each other. The nonparametric tests compute several test statistics to determine if two set of data are samples of the same distribution. All the statistics methods are implemented in the stats sub-package of the SciPy library in Python (https://scipy.org), more details about these methods in [24]–[26].

The p-value computed by a statistical test is the probability of type I error, that is the probability of rejecting the null

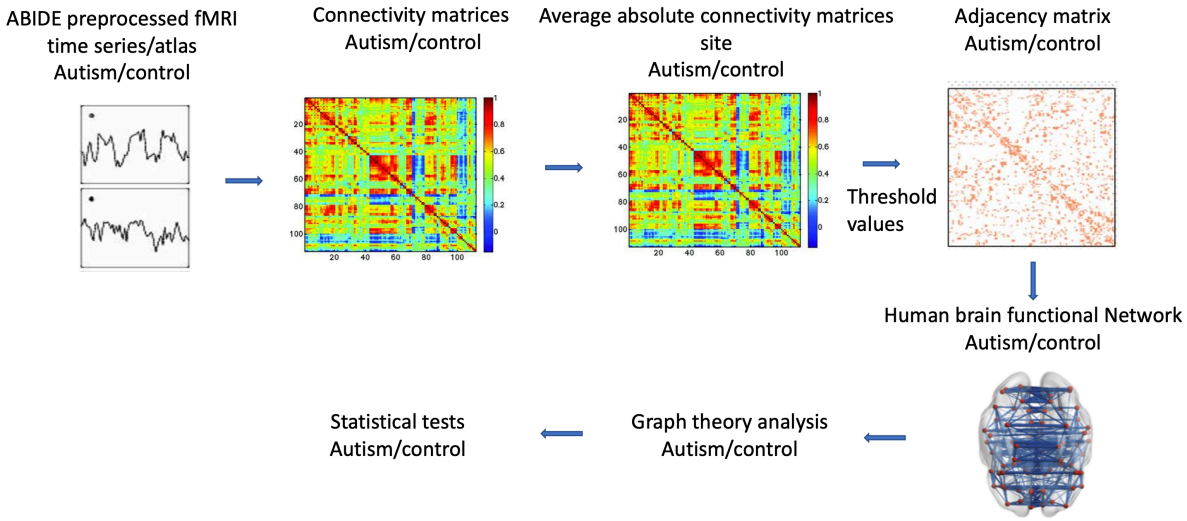

Fig. 1: Pipeline to perform the statistical analysis of the graph theory measures computed from the human brain functional networks representing the ABIDE rest-fMRI preprocessed data obtained from the control and autism subjects.

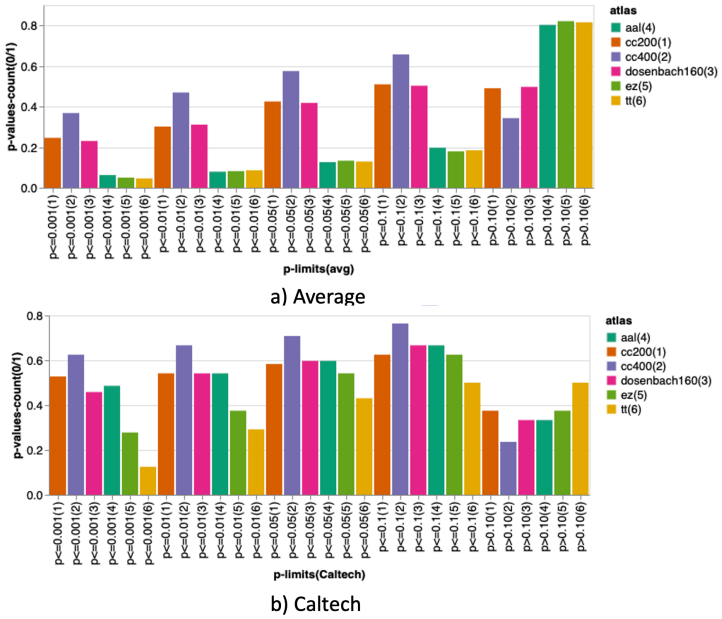

Fig. 2: Histograms of the normalized p-values-counts for the intervals $p \leq 0.001$, $p \leq 0.01$, $p \leq 0.05$, $p \leq 0.1$, and $p > 0.1$, obtained from the average of these values corresponding to each atlas. The a) Average histogram shows the average for all sites of the p-values-counts intervals, while the b) Caltech histogram shows the same information for the Caltech site.

hypothesis H_0 when H_0 is true, where in this paper H_0 is the hypothesis that the graph measures of the autism and control functional graphs are from the same distribution. The p-value is also known as the observed level of significance. The smaller the p-value, the more significant is the statistical test result [24]. In order to classify the statistical test results, four significance levels: $0.001, 0.01, 0.05, 0.1$ were defined for the p-values, that resulted in the following five intervals: $p \leq 0.001$, $p \leq 0.01$, $p \leq 0.05$, $p \leq 0.1$, and $p > 0.1$. These p-values intervals were used to classify the statistical tests results obtained for example for a graph measure, by counting the number of times the p-values fall in a particular interval. The greater the number of p-values counted in the first four intervals, the greater the capability of the graph measure to detect statistical differences between the measures computed for the graphs representing control and autism subjects.

III. Results.

The average of all the statistics tests results corresponding to each atlas was computed for each imaging site, obtaining

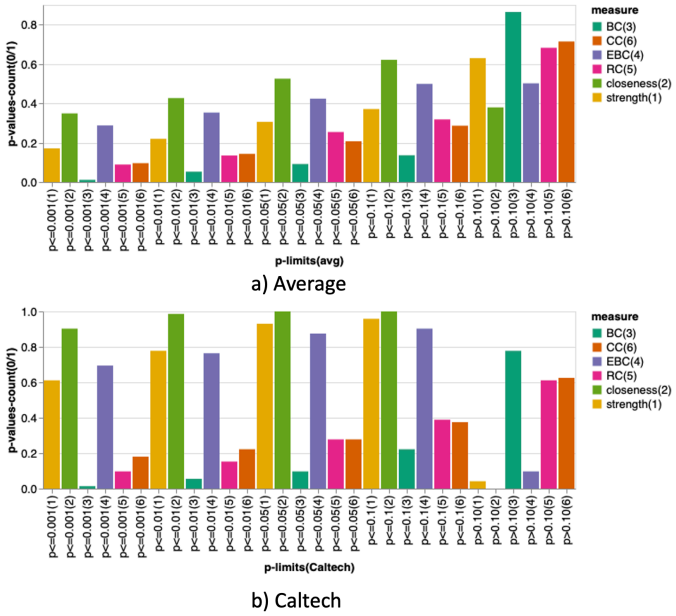

Fig. 3: Histograms of the normalized p-values-counts for the intervals $p \leq 0.001$, $p \leq 0.01$, $p \leq 0.05$, $p \leq 0.1$, and $p > 0.1$, obtained from the average of these values obtained for each graph measure. The a) Average histogram shows the average for all sites of the p-values-counts intervals, while the b) Caltech histogram shows the same information for the Caltech site.

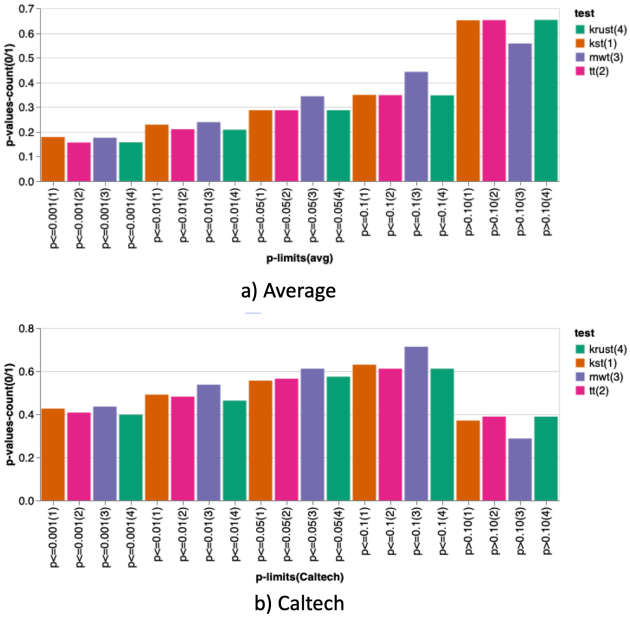

Fig. 4: Histograms of the normalized p-values-counts for the intervals $p \leq 0.001$, $p \leq 0.01$, $p \leq 0.05$, $p \leq 0.1$, and $p > 0.1$, obtained from the average of these values obtained for each statistical test. The a) Average histogram shows the average for all sites of the p-values-counts intervals, while the b) Caltech histogram shows the same information for the Caltech site.

the normalized p-values counts for the intervals $p \leq 0.001$, $p \leq 0.01$, $p \leq 0.05$, $p \leq 0.1$, and $p > 0.1$, for each atlas per imaging site. The histogram of Figure 2 b) shows these results for the Caltech site. To facilitate the reading of this Figure, the numbers between brackets map each p-value interval with the corresponding atlas.

The average of the averages of the p-values per site, were computed to obtain global averages of the p-values counts values corresponding to all the fMRI data provided for the ten imaging sites of Table I. The histogram of Figure 2 a) shows these global results.

Figures 3, 4, and 5 show similar results for the normalized

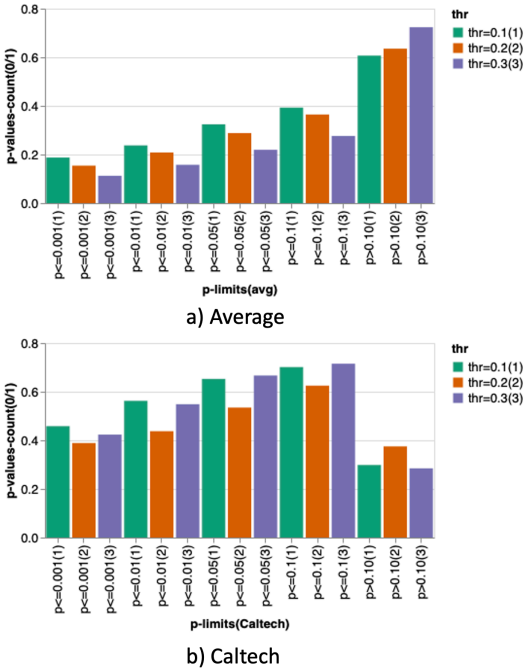

Fig. 5: Histograms of the normalized p-values-counts for the intervals $p \leq 0.001$, $p \leq 0.01$, $p \leq 0.05$, $p \leq 0.1$, and $p > 0.1$, obtained from the average of these values corresponding to the sparse graphs for each threshold value. The a) Average histogram shows the average for all sites of the p-values-counts intervals, while the b) Caltech histogram shows the same information for the Caltech site.

p-values counts for the graph measures, for the statistical tests, and for the sparse graphs corresponding to the selected threshold values respectively.

Al the results presented in this section are easily reproducible since the fMRI data and the software packages used for computing them are publicly available.

IV. Discussion

The results shown in Figure 2 a), demonstrated that the level of significance of the statistical analysis of the graph measures are strongly dependent on the type of atlas used as brain parcellations. These results also showed that the level of significance obtained with the atlases derived from functional data, i.e., cc200, cc400, and dosenbach160 are, in average, much higher than the corresponding levels of significance of the anatomical derived atlases. The highest level of significance was obtained with the cc400 atlas. The results obtained for the Caltech site (Figure 2 b)) showed levels of significance much higher than the global average, also showing much better results for the anatomical derived atlases, especially those corresponding to the Automated Anatomical Labeling (aal) atlas.

The high level of significance obtained for the graph theory measures: strength, closeness centrality, and edge betweenness centrality (EBC) (Figure 3 a)) showed a strong dependence of the corresponding results of the functional network statistical analysis on these measures. These results were confirmed by the level of significance obtained for these measures with the Caltech site fMRI data (Figure 3 a)), which are much higher than the corresponding global average.

The levels of significance corresponding to the statistical tests methods (Figure 4 a)) are on average similar among the tests, with the Mann–Whitney U test (mwt) showing the highest level of significance. This result was confirmed by the corresponding level of significance obtained for the Caltech site (Figure 4 b)), which are much higher than the average values. These results also confirmed the consistency of the statistical tests methods used in this research. The levels of significance corresponding to the sparse graphs obtained with the selected threshold values are also very homogeneous, especially those corresponding to the threshold values 0.1 and 0.2 (Figure 5). These results showed that the functional network statistical analysis results are less dependent on the statistical tests methods, and on the threshold values applied to the connectivity matrices to obtain the adjacency matrices of the sparse graphs.

The higher levels of significance showed for the Caltech site compared to the average case suggested that the best results on the statistical analysis of functional human brain networks are obtained when the source of the fMRI data is the same for all the data.

V. Conclusion and Future Work

In order to improve and enhance the scope of the methods presented here, we will incorporate brain parcellations directly computed from the fMRI data using decomposition methods

such as Independent Component Analysis (ICA) [7], which will complement the statistical results obtained with the atlases included in this paper. We also will improve the methods to compute the sparse graphs by selecting thresholds for which the graphs, representing autism and control subjects, have the same density and the same number of edges, improving therefore the statistical comparison of the corresponding graph measures. The results of this research will be presented in a paper which is under preparation.

Machine learning, especially deep learning, techniques have been widely used in network neuroscience research for the diagnosis of mental disorders by accurately classifying patients with these type of disorders [27]. Considering the promising future and high potential of success of this area of research, our future work will be focused on improving our methodology by incorporating machine learning techniques to perform functional network statistical analysis, in order to determine the main factors that strongly affect the reproducibility and reliability of the results of this analysis.

Since reproducibility and reliability of functional brain network statistical analysis is strongly dependent on the type of fMRI data, brain parcellations, and graph theory measures; our expectation is that the novel results presented in this paper would further help researchers in this field to develop standard workflows to perform reliable and reproducible functional networks analysis, that may be adapted by the neuroscience community.

VI. Acknowledgements

This research was supported by the National Science Foundations (NSF) under the Award Numbers CAREER OAC-1925960 and NIH R01GM134384. The content is solely the responsibility of the authors and does not necessarily represent the official views of the National Science Foundation. We would also like to acknowledge the donation of a K-40c Tesla GPU and a TITAN Xp GPU from NVIDIA which was used for all the GPU-based experiments performed in this paper.

References

[1] D. S. Bassett and O. Sporns, "Network neuroscience," *Nature Neuroscience*, vol. 20, no. 3, pp. 353–364, 2017. [Online]. Available: https://doi.org/10.1038/nn.4502

[2] E. T. Bullmore and D. S. Bassett, "Brain graphs: Graphical models of the human brain connectome," *Annual Review of Clinical Psychology*, vol. 7, no. 1, pp. 113–140, 2011, pMID: 21128784. [Online]. Available: https://doi.org/10.1146/annurev-clinpsy-040510-143934

[3] O. Sporns, "From simple graphs to the connectome: Networks in neuroimaging," *NeuroImage*, vol. 62, no. 2, pp. 881–886, 2012, 20 YEARS OF fMRI. [Online]. Available: https://www.sciencedirect.com/science/article/pii/S1053811911010172

[4] S. B. Eickhoff, B. T. Yeo, and S. Genon, "Imaging-based parcellations of the human brain," *Nature Reviews Neuroscience*, vol. 19, no. 11, pp. 672–686, 2018.

[5] Z. Wu, D. Xu, T. Potter, Y. Zhang, A. D. N. Initiative *et al.*, "Effects of brain parcellation on the characterization of topological deterioration in alzheimer's disease," *Frontiers in aging neuroscience*, vol. 11, p. 113, 2019.

[6] M. Salehi, A. S. Greene, A. Karbasi, X. Shen, D. Scheinost, and R. T. Constable, "There is no single functional atlas even for a single individual: Functional parcel definitions change with task," *NeuroImage*, vol. 208, p. 116366, 2020.

[7] Q. Yu, Y. Du, J. Chen, J. Sui, T. Adalē, G. D. Pearlson, and V. D. Calhoun, "Application of graph theory to assess static and dynamic brain connectivity: Approaches for building brain graphs," *Proceedings of the IEEE*, vol. 106, no. 5, pp. 886–906, 2018.

[8] M. Rubinov and O. Sporns, "Complex network measures of brain connectivity: uses and interpretations," *Neuroimage*, vol. 52, no. 3, pp. 1059–1069, 2010.

[9] E. Bullmore and O. Sporns, "Complex brain networks: graph theoretical analysis of structural and functional systems," *Nature reviews neuroscience*, vol. 10, no. 3, pp. 186–198, 2009.

[10] X.-N. Zuo, R. Ehmke, M. Mennes, D. Imperati, F. X. Castellanos, O. Sporns, and M. P. Milham, "Network centrality in the human functional connectome," *Cerebral cortex*, vol. 22, no. 8, pp. 1862–1875, 2012.

[11] A. Fornito, A. Zalesky, and E. Bullmore, *Fundamentals of brain network analysis*. Academic Press, 2016.

[12] P. Tewarie, E. van Dellen, A. Hillebrand, and C. J. Stam, "The minimum spanning tree: an unbiased method for brain network analysis," *Neuroimage*, vol. 104, pp. 177–188, 2015.

[13] S. Noble, D. Scheinost, and R. T. Constable, "A decade of test-retest reliability of functional connectivity: A systematic review and meta-analysis," *Neuroimage*, vol. 203, p. 116157, 2019.

[14] C. Craddock, Y. Benhajali, C. Chu, F. Chouinard, A. Evans, A. Jakab, B. S. Khundrakpam, J. D. Lewis, Q. Li, M. Milham *et al.*, "The neuro bureau preprocessing initiative: open sharing of preprocessed neuroimaging data and derivatives," *Frontiers in Neuroinformatics*, vol. 7, 2013.

[15] R. C. Craddock, G. A. James, P. E. Holtzheimer III, X. P. Hu, and H. S. Mayberg, "A whole brain fmri atlas generated via spatially constrained spectral clustering," *Human brain mapping*, vol. 33, no. 8, pp. 1914–1928, 2012.

[16] N. U. Dosenbach, B. Nardos, A. L. Cohen, D. A. Fair, J. D. Power, J. A. Church, S. M. Nelson, G. S. Wig, A. C. Vogel, C. N. Lessov-Schlaggar *et al.*, "Prediction of individual brain maturity using fmri," *Science*, vol. 329, no. 5997, pp. 1358–1361, 2010.

[17] N. Tzourio-Mazoyer, B. Landeau, D. Papathanassiou, F. Crivello, O. Etard, N. Delcroix, B. Mazoyer, and M. Joliot, "Automated anatomical labeling of activations in spm using a macroscopic anatomical parcellation of the mni mri single-subject brain," *Neuroimage*, vol. 15, no. 1, pp. 273–289, 2002.

[18] S. B. Eickhoff, K. E. Stephan, H. Mohlberg, C. Grefkes, G. R. Fink, K. Amunts, and K. Zilles, "A new spm toolbox for combining probabilistic cytoarchitectonic maps and functional imaging data," *Neuroimage*, vol. 25, no. 4, pp. 1325–1335, 2005.

[19] J. Talairach, "Atlas d'anatomie stéréotaxique du télencéphale: etudes anatomo-radiologiques; atlas of stereotaxic anatomy of the telencephalon," 1967.

[20] A. C. Evans, A. L. Janke, D. L. Collins, and S. Baillet, "Brain templates and atlases," *Neuroimage*, vol. 62, no. 2, pp. 911–922, 2012.

[21] Z. Yao, B. Hu, Y. Xie, P. Moore, and J. Zheng, "A review of structural and functional brain networks: small world and atlas," *Brain informatics*, vol. 2, no. 1, pp. 45–52, 2015.

[22] A. Hagberg, P. Swart, and D. S Chult, "Exploring network structure, dynamics, and function using networkx," Los Alamos National Lab.(LANL), Los Alamos, NM (United States), Tech. Rep., 2008.

[23] M. Newman, *Networks*. Oxford university press, 2018.

[24] A. Tamhane and D. Dunlop, "Statistics and data analysis: from elementary to intermediate," 2000.

[25] G. W. Corder and D. I. Foreman, *Nonparametric statistics: A step-by-step approach*. John Wiley & Sons, 2014.

[26] P. Sprent and N. C. Smeeton, *Applied nonparametric statistical methods*. CRC press, 2016.

[27] T. Eslami, F. Almuqhim, J. S. Raiker, and F. Saeed, "Machine learning methods for diagnosing autism spectrum disorder and attention-deficit/hyperactivity disorder using functional and structural mri: A survey," *Frontiers in Neuroinformatics*, vol. 14, p. 62, 2021. [Online]. Available: https://www.frontiersin.org/article/10.3389/fninf.2020.575999